One-pot, large-scale synthesis of SnO_2 nanotubes at room temperature†

Ning Du, Hui Zhang, Bingdi Chen, Xiangyang Ma and Deren Yang*

Received (in Cambridge, UK) 9th January 2008, Accepted 13th March 2008
First published as an Advance Article on the web 21st April 2008
DOI: 10.1039/b800401c

SnO_2 Nanotubes were synthesized *via* a one-pot redox route at room temperature, in which the Kirkendall effect is definitely responsible for the formation of hollow structures.

The Kirkendal effect has long been known to result in porosity or deformation in the case of alloying or oxidation of metals, because the mutual diffusion rates of two components in a diffusion couple differ by a considerable amount.[1] Since the first report of hollow nanocrystals formed through the nanoscale Kirkendall effect by Alivisatos *et al.*,[2] considerable efforts have been expended on the preparation of hollow nanostructures based on the this effect.[3–15] For example, hollow Fe_3O_4 nanocrystals were prepared through the controlled oxidation of core-shell Fe–Fe_3O_4 nanoparticles in the presence of oxygen-transfer reagent trimethylamine *N*-oxide (Me_3NO).[3] Ag_2Se nanotubes were synthesized by ultraviolet (UV) photodissociation of the adsorbed CSe_2 on the surface of Ag nanowires under ambient condition.[4] However, few papers reported on the fabrication of metal oxide nanotubes through the Kirkendall effect.[5] Generally, metal oxide nanotubes were synthesized by rolling up layered materials, eliminating the core of core-shell nanowires, or removable template assisted deposition.[16] Recently, single crystalline $ZnAl_2O_4$ spinel nanotubes have been fabricated through the solid-state reaction of core-shell ZnO–Al_2O_3 nanowires at 700 °C.[5]

In this letter, we report on the synthesis of SnO_2 nanotubes *via* a one-pot redox route at room temperature, in which the Kirkendall effect is definitely responsible for the formation of hollow structures. In our strategy, the formation of Sn nanorods as the template and the reaction proceed consecutively in the same precursor solution, unlike the cases in the previous reports where the templates were separately synthesized prior to being involved in the Kirkendall effect mediated reaction. It should be mentioned that the SnO_2 nanostructured material chosen in this work has attracted great attention in recent years for the promising applications in sensor, energy storage and optoelectronics.[17–19]

Briefly, the Sn nanorods were firstly formed by the reduction of Sn^{4+} ions using PDDA (poly diallyldimethylammonium choride) as soft template, which were subsequently oxidized into SnO_2 nanotubes at room temperature (Fig. 1a). In our strategy, the synthesis of the Sn nanorods at the initial stage of the reaction determined the subsequent formation of the SnO_2 nanotubes. Moreover, the linear cationic PDDA, which was usually used in the layer-by-layer assembly process for synthesizing nanocomposites,[20–22] was considered to play the most important role in the formation of Sn nanorods. The role of PDDA was similar to that of CTAB (cetyltrimethylammonium bromine), which could organize into rod-shaped micelles and acted as soft template to promote the formation of nanorods.[23] In our strategy, the negatively charged BH_4^- was adsorbed on the surface of the rod-shaped micelles of PDDA due to the electrostatic attraction between the charged species. Therefore, the deoxidization of Sn^{4+} to Sn by BH_4^- took place in the channel of the rod-shaped micelles, resulting in the formation of Sn nanorods. In the absence of PDDA, Sn nanoparticles could be quickly oxidized into SnO_2 nanoparticles, and no Sn nanorods were formed (Fig. S1†). In addition, no Sn nanorods were formed (Fig. S2†) when the negatively charged PSS (poly sodium 4-styrenesulfonate) replaced PDDA as the soft template in the reaction, indicating that the electrostatic attraction between the negatively charged BH_4^- and positively charged PDDA played the critical role in the formation of the Sn nanorods.

Fig. 1b and c show the evolution of the solution color and the corresponding X-ray diffraction patterns (XRD) along with the reaction time. The color of the solution was black-brown when the reaction proceeded for 5 min. The corresponding XRD pattern only reveals the peaks assigned to

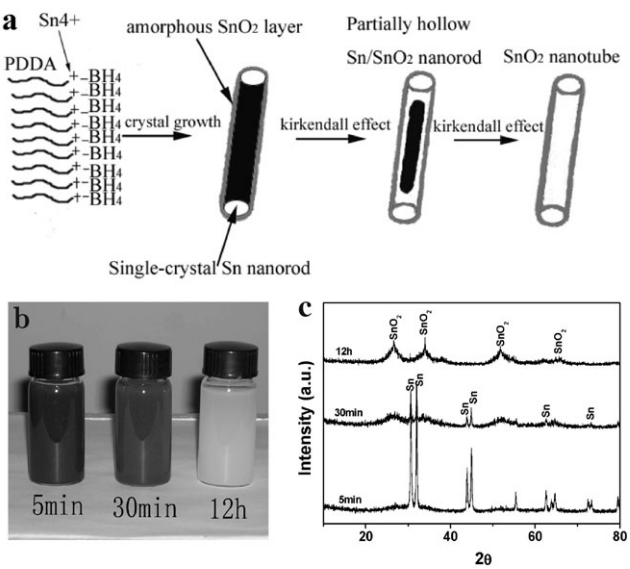

Fig. 1 (a) Schematic diagram for the growth process of SnO_2 nanotubes. (b) Color change from Sn nanorods to SnO_2 nanotubes with the prolonged reaction time (5 min, 30 min, 12 h); (c) XRD patterns of the corresponding products as shown in (b).

State Key Lab of Silicon Materials and Department of Materials Science and Engineering, Zhejiang University, Hangzhou, 310027, People's Republic of China. E-mail: mseyang@zju.edu.cn; Fax: +86-571-87952322; Tel: +86-571-87951667

† Electronic supplementary information (ESI) available: Experimental detail, TEM and XPS results. See DOI: 10.1039/b800401c

tetragonal Sn (JCPDS 01-0926), indicating the formation of the pure Sn phase at the initial stage. After 30 min reaction, the color of the solution turned to beige, and the peaks of SnO_2 emerged in the corresponding XRD pattern. This represents the partial oxidation of Sn into SnO_2. After 12 h reaction, the color of solution turned to be fairly white (sometime a little yellow) and all the peaks of the corresponding XRD pattern could be assigned to tetragonal SnO_2 (JCPDS 03-1114), which indicates the complete transformation from Sn to SnO_2. In a word, the evolution of the XRD pattern in combination with the color transformation of the solution clearly demonstrates the phase transformation from Sn to SnO_2.

Transmission electron microscopy (TEM) analysis was employed to further demonstrate the phase transformation process as described above. Fig. 2a is a TEM image of the product obtained with a reaction time of 5 min, exhibiting the nanorods with the diameters of 30–50 nm and the lengths of 300–500 nm. Moreover, some shorter nanorods can also be found, which may be due to the uneven molecular weight (10 000–30 000) of PDDA. Fig. 2b shows the high-resolution transmission electron microscopy (HRTEM) image of an individual Sn nanorod. The interlayer spacings of 0.29 nm and 0.28 nm correspond well to the *d*-spacings of the (200) and (101) planes of bulk metal Sn, respectively. In addition, the corresponding selected area electron diffraction pattern (SAED) is shown in the bottom right inset of Fig. 2b, indicating the [001] growth direction and single-crystalline nature of the Sn nanorods as shown in Fig. 2a. However, a nearly amorphous SnO_2 layer with a thickness of 3–5 nm can be seen from the HRTEM image, because the Sn nanorods synthesized at the initial stage of the reaction were not chemically stable, and were partially oxidized when exposed to the air during the reaction.

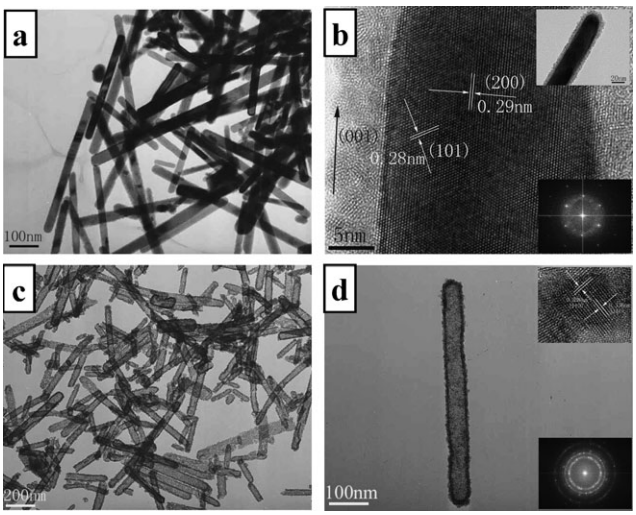

Fig. 2 (a) TEM image of the as-synthesized Sn nanorods obtained with the reaction time of 5 min; (b) HRTEM image of an individual Sn nanorod with right-upper inset image of TEM image and right-down SAED pattern; (c) the as-synthesized SnO_2 nanotubes obtained with the reaction time of 12 h; (d) TEM image of an individual SnO_2 nanotube with right-up inset HRTEM image and right-down SAED pattern.

Moreover, the initial oxidized layer was considered to be the key factor for the formation of the hollow structure because this layer could facilitate the unbalanced interfacial diffusion of O and Sn atoms during the oxidation process.[3]

Fig. 2c shows the TEM image of the product obtained with the reaction time of 12 h, illustrating as the nanotubes with the diameters of 50–60 nm and the lengths of 300–500 nm. This further confirms the transformation from the nanorods to the nanotubes with the prolonged reaction time. Moreover, a 10–20 nm increase in the diameter of SnO_2 nanotubes compared with that of starting Sn nanorods can be seen as a result of the outward flow of Sn during the oxidation. Further characterization of an individual SnO_2 nanotube is shown in Fig. 2d. A high contrast between the bright central part and two dark edges demonstrates the hollow characteristic of the tube. The right-upper inset in Fig. 2d is the HRTEM image of an individual SnO_2 nanotube. There is the same *d* value of 0.34 nm in the two grains corresponds to the (110) plane of SnO_2, indicating the polycrystalline nature of SnO_2 nanotubes, which is further confirmed by the inset SAED pattern. In general, the structure of tube-organized nanoparticles with high surface area may show superior performance in sensor and lithium-ion-battery.[22,24] Furthermore, the length of SnO_2 nanotubes can be readily controlled by the addition of different amounts of PDDA (Fig. S3†). With the increased volume of PDDA from 0.1 to 2 ml, the lengths of the Sn nanorods and SnO_2 nanotubes vary from a few tens to hundreds of nanometres.

To illusatrate the evolution from the Sn–SnO_2 core-shell nanorods to the SnO_2 nanotubes during the oxidation process, the product obtained with a reaction time of 30 min was characterized by TEM, HRTEM and XPS. Fig. 3a shows the TEM image of the obtained product. As can be seen, the product manifests itself as the hollow Sn–SnO_2 nanorods. Fig. 3b–e show the four cases of partially hollow Sn–SnO_2 nanorods with different hollow formation. Fig. 3b exhibits a gap between the Sn core and SnO_2 layer formed during the oxidation process, which is similar to the void formation inside the nanocrystals.[2,3] Moreover, some Sn bridges can also be seen between the shell and core, which is similar to the observation in the synthesis of CoS and Fe_3O_4 hollow nanocrystals.[2,3] These bridges seem to provide the fast transport path for outward diffusion Sn atoms that can then spread on the inner shell surface. However, Fig. 3c–e show the uneven hollow formation. For spherical nanocrystal system, the conventional Kirkendall-type diffusion model employs a one-dimensional steady state bulk flux governed by Fick's first

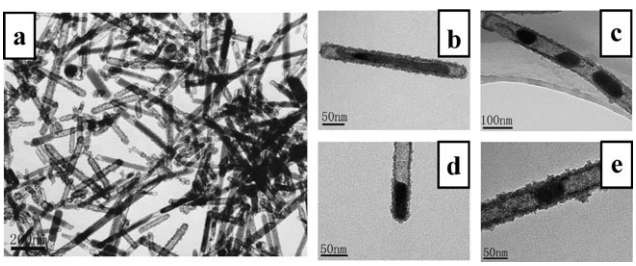

Fig. 3 TEM images: (a) the as-synthesized Sn–SnO_2 partially hollow nanotubes obtained with the reaction time of 30 min; (b–e) four different forms of Sn–SnO_2 partially hollow nanotubes.

law and the hollow formation was even between the core and shell during the reaction. For one-dimensional system, the Kirkendall effect combined with the surface diffusion mechanism has recently been presented through investigating the formation of $ZnAl_2O_4$ nanotubes, in which the uneven flux of inner constituent in the cylindrical coordination easily happens.[8] This is also the case in our experiment. The uneven flux of inner constituent may induce the uneven hollow formation between the Sn core and SnO_2 layer. Further HRTEM characterization of the interface between Sn and SnO_2 was shown in Fig. S4.† Two different interlayer spacings of 0.29 and 0.34 nm correspond to the *d*-spacing of (200) plane of Sn and (110) plane of SnO_2, indicating the coexistence of Sn and SnO_2. The above TEM observations made in the process of forming hollow SnO_2 nanotubes reveal that the Kirkendall effect dictates the oxidation of Sn nanorods, in which the metal Sn diffuses faster outward than oxygen does inward. This is consistent with the observation that the metal is the faster diffusing component in a diffusion couple of metal and oxygen.[25]

The XPS analysis of the Sn–SnO_2 partially hollow nanorods as shown in Fig. 3 was also shown (Fig. S5†). The measured elements are tin (Sn 3s, 3p, 3d, 4s, 4p, 4d), oxygen (O1s), sodium (Na1s), nitrogen (1s) and chlorine (Cl 1s, 2p). The peak at 486.59 eV corresponds to Sn $3d_{5/2}$ of Sn^{4+} and a small peak with a binding energy of 484.35 eV could be separated from the Sn $3d_{5/2}$ of Sn^{4+}, which corresponds to the Sn $3d_{5/2}$ state of metal Sn, indicative of the coexistence of Sn^{4+} and metal Sn.[26–28] Moreover, SnO_2 is a predominant phase in the Sn/SnO_2 partially hollow nanorods as confirmed by the XPS analysis, which is consistent with the TEM characterization (Fig. 3). In addition, the peaks of sodium, nitrogen and chlorine originate from the PDDA, indicating the existence of PDDA on the surface of SnO_2 shell.

Regarding the previous syntheses of hollow nanocrystals based on the Kirkendall effect, they can be described as the following two steps: (1) separately synthesis solid nanocrystals as the template; (2) application of the template in the subsequent reaction to form hollow nanocrystals. While, in our experiment, the reacting template of Sn nanorods formed at the very beginning of the reaction could gradually turn into the SnO_2 nanotubes along with the extended reaction time. It is thus indicated that the generally adopted two-step strategy for the synthesis of hollow nanostructure can be simplified as a one-pot route through our present strategy.

In conclusion, we have succeeded in preparing SnO_2 nanotubes through a mild wet-chemistry route at room temperature involving the Kirkendall effect. The reactive template of Sn nanorods was initially formed by a redox reaction using PDDA as the soft template, which then gradually turned into SnO_2 nanotubes along with the extension of reaction time. Moreover, the present strategy is expected to be extended to synthesize other metal oxide nanotubes.

The authors would like to appreciate the financial supports from Program for Changjiang Scholar and Innovative Team in University, Program 973 (No. 2007CB613403), ZiJin Project, Zhejiang Provincial Natural Science Foundation of China (Y407138) and Doctoral Program of Ministry of Education of China (No. 20070335014). Thanks Prof. Youwen Wang and Yuewu Zeng for the TEM measurements

Notes and references

1. A. D. Smigelskas and E. O. Kirkendall, *Trans. AIME*, 1947, **171**, 130.
2. Y. D. Yin, R. M. Rioux, C. K. Erdonmez, S. Hughes, G. A. Somorjai and A. P. Alivisato, *Science*, 2004, **304**, 711.
3. S. Peng and S. Sun, *Angew. Chem., Int. Ed.*, 2007, **46**, 1.
4. H. J. Fan, M. Knez, R. Scholz, K. Nielsch, E. Pippel, D. Hesse, M. Zacharias and U. Gosele, *Nat. Mater.*, 2006, **5**, 631.
5. C. H. Bernard, H. Tan and W. Y. Fan, *Langmuir*, 2006, **22**, 9712.
6. B. Liu and H. C. Zeng, *J. Am. Chem. Soc.*, 2004, **126**, 16744.
7. Q. G. Li and R. M. Penner, *Nano Lett.*, 2005, **5**, 1720.
8. H. J. Fan, M. Knez, R. Scholz, D. Hesse, K. Nielsch, M. Zacharias and U. Gosele, *Nano Lett.*, 2007, **7**, 933.
9. K. N. Tu and U. Gosele, *Appl. Phys. Lett.*, 2005, **86**, 093111.
10. H. Tan, S. P. Li and W. Y. Fan, *J. Phys. Chem. B*, 2006, **110**, 15812.
11. A. E. Henkes, Y. Vasquez and R. E. Schaak, *J. Am. Chem. Soc.*, 2007, **129**, 1896.
12. Y. D. Yin, C. K. Erdonmez, A. Cabot, S. Hughes and A. P. Alivisatos, *Adv. Funct. Mater.*, 2006, **16**, 1389.
13. H. L. Cao, X. F. Qian, J. T. Zai, J. Yin and Z. K. Zhu, *Chem. Commun.*, 2006, 4548.
14. Y. L. Wang, L. Cai and Y. N. Xia, *Adv. Mater.*, 2005, **17**, 473.
15. Y. D. Yin, C. Erdonmez, S. Aloni and A. P. Alivisatos, *J. Am. Chem. Soc.*, 2006, **128**, 12671.
16. C. N. R. Rao and M. Nath, *Dalton Trans.*, 2003, 1–24.
17. Y. Idota, T. Kubota, A. Matsufuji, Y. Maekawa and T. Miyasaka, *Science*, 1997, **276**, 1395.
18. M. Law, H. Kind, F. Kim, B. Messer and P. Yang, *Angew. Chem., Int. Ed.*, 2002, **41**, 2405.
19. C. Tatsuyama and S. Ichimura, *Jpn. J. Appl. Phys.*, 1976, **15**, 843.
20. G. Decher, *Science*, 1997, **277**, 1232.
21. Z. Y. Tang, N. A. Kotov, S. Magonov and B. Ozturk, *Nat. Mater.*, 2003, **2**, 413.
22. N. Du, H. Zhang, B. D. Chen, X. Y. Ma, Z. L. Liu, J. B. Wu and D. Yang, *Adv. Mater.*, 2007, **19**, 1641.
23. Y. N. Xia, P. D. Yang, Y. G. Sun, Y. Y. Wu, B. Mayers, B. Gates, Y. D. Yin, F. Kim and H. Q. Yan, *Adv. Mater.*, 2003, **15**, 353.
24. Y. Wang, H. C. Zeng and J. Y. Lee, *Adv. Mater.*, 2006, **18**, 645.
25. G. W. Leibbrandt, G. Hoogers and F. H. P. M. Habraken, *Phys. Rev. Lett.*, 1992, **68**, 1947.
26. H. J. Ahn, H. C. Choi, K. W. Park, S. B. Kim and Y. E. Sun, *J. Phys. Chem. B*, 2004, **108**, 9815–9820.
27. S. H. Luo, P. K. Chu and Z. F. Di, *Appl. Phys. Lett.*, 2006, **88**, 013109.
28. K. R. Hallam and R. K. Wild, *Surf. Interface Anal.*, 2004, **23**, 133.

